A new Cd(II)-based MOF displaying flu topology as a highly sensitive and selective photoluminescent sensor for ferric and chromate ions

Xue Lan,[a] Li Yang,[b] Jun Wang[a], Lu Lu,[a,*] Mohd. Muddassir,[c] Devyani Srivastava,[d] Aparna Kushwaha,[d] Abhinav Kumar,[d*] Ying Pan,[e,*]

a.School of Chemistry and Environmental Engineering, Sichuan University of Science & Engineering, Zigong 643000, PR. China. E-mail: lulu2004770@suse.edu.cn, Tel/Fax: +86-0813-5505605
b.Key Laboratory of Low-cost Rural Environmental Treatment at Sichuan Unviersity of Arts and Science, Education Department of Sichuan Province, 635000, PR. China
c.Department of Chemistry, College of Sciences, King Saud University, Riyadh 11451, Saudi Arabia.
d.Department of Chemistry, Faculty of Science, University of Lucknow, Lucknow 226 007, India. E-mail: abhinavmarshal@gmail.com
[e]Dongguan Key Laboratory of Drug Design and Formulation Technology, School of Pharmacy, Guangdong Medical University, Guangdong Medical University Key Laboratory of Research and Development of New Medical Materials, Dongguan, 523808, China E-mail: panying@gdmu.edu.cn

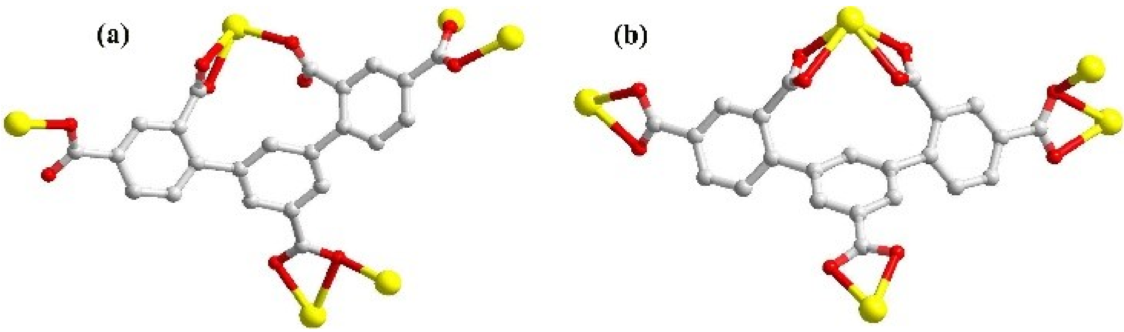

Scheme S1. Different coordination modes of 3,5-di(2’,4’-dicarboxylphenyl)benozoic acid ligand

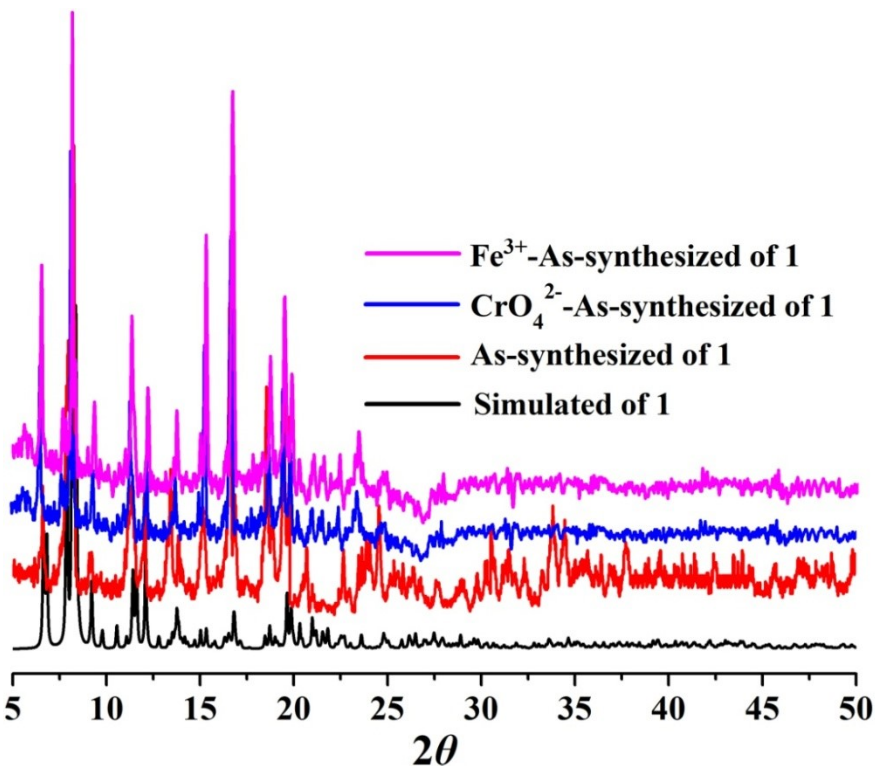

Fig. S1 PXRD plots for **1** in different conditions.

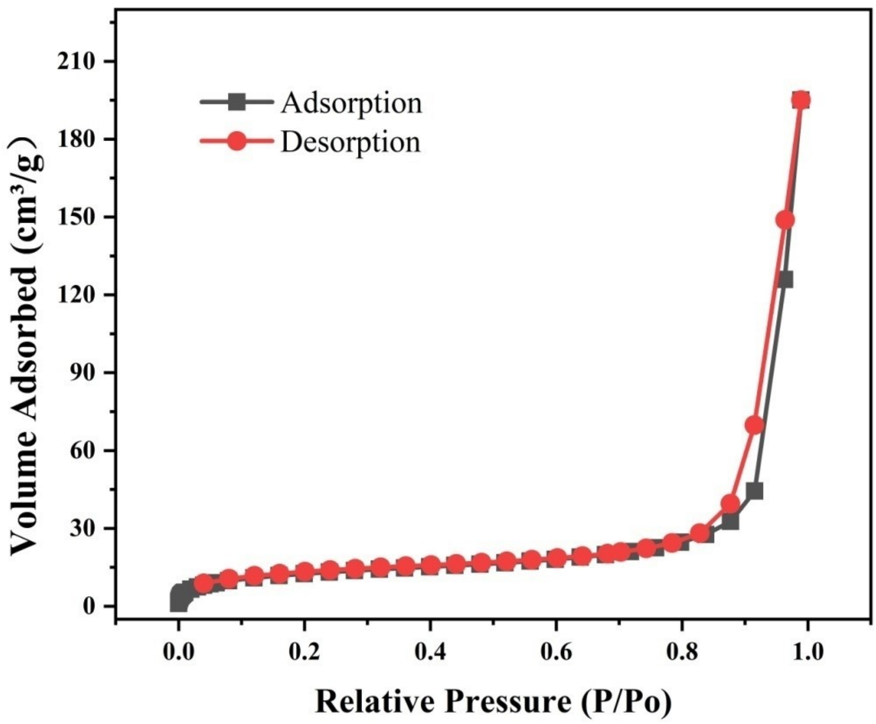

Fig. S2 Nitrogen adsorption- desorption isotherm of **1**.

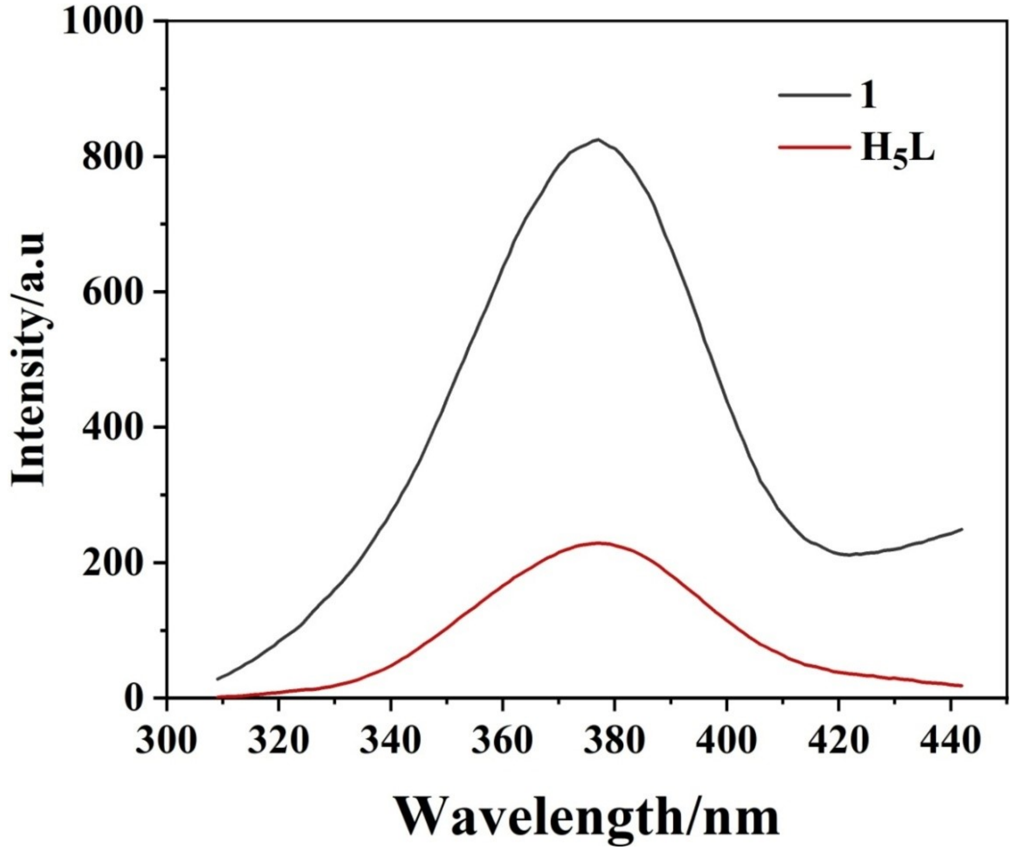

Fig. S3 Photoluminescence spectra of **1** and H_5L ligand.

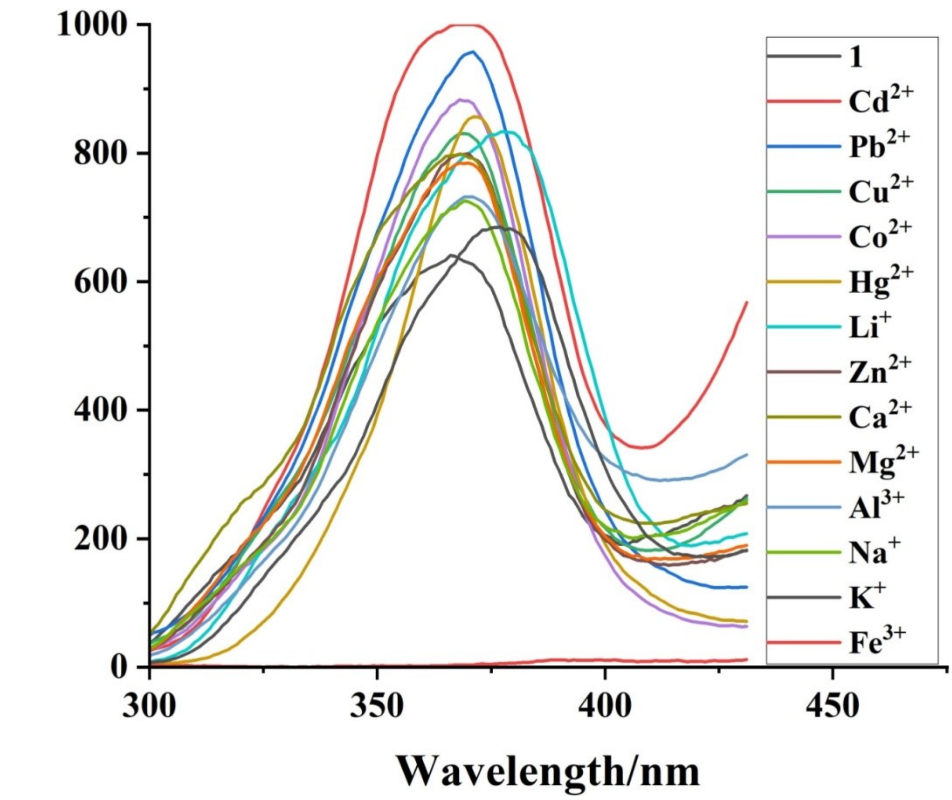

Fig. S4 Photoluminescence spectra of **1** in the presence of different anions.

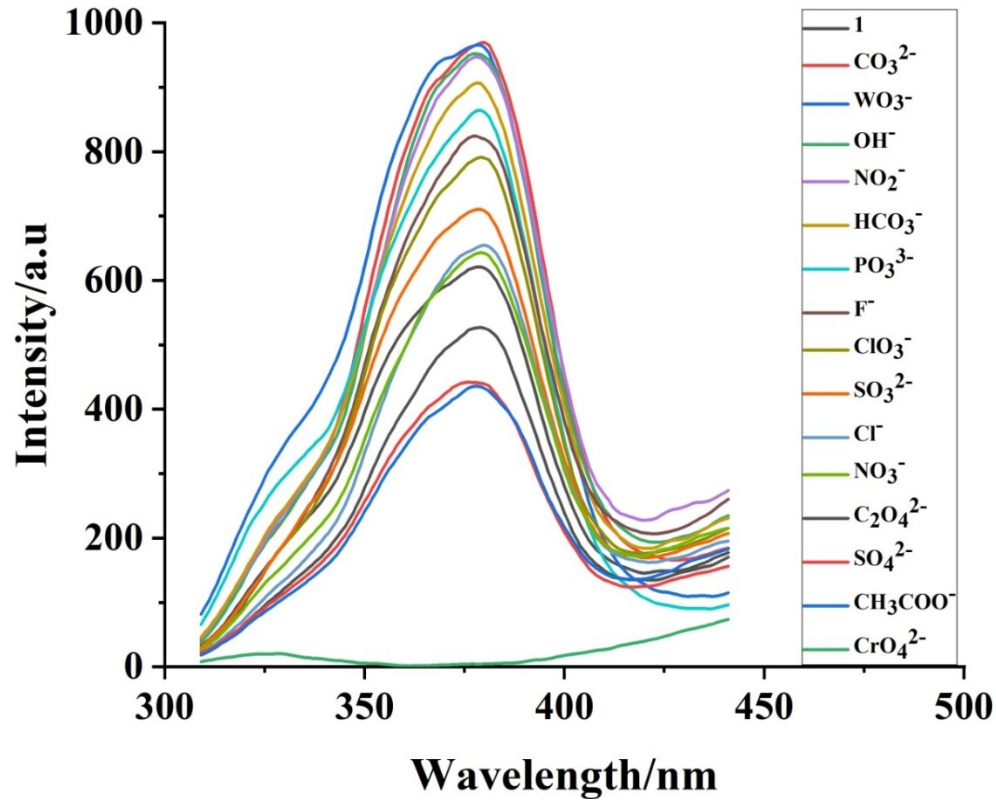

Fig. S5 Plot representing decline in emission intensity of **1** in the presence of different metal anions.

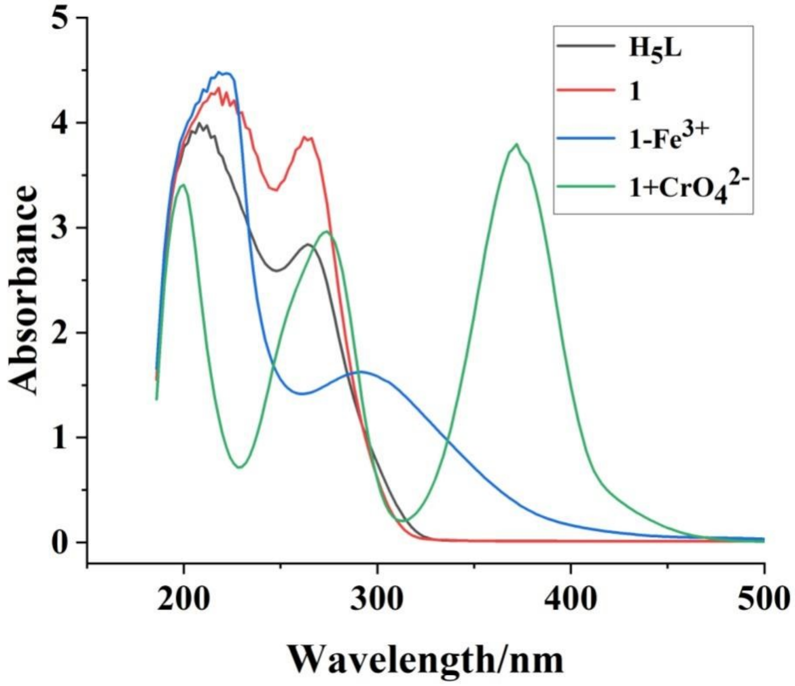

Fig. S6 the UV–Vis absorption spectra of tested cations and anions.

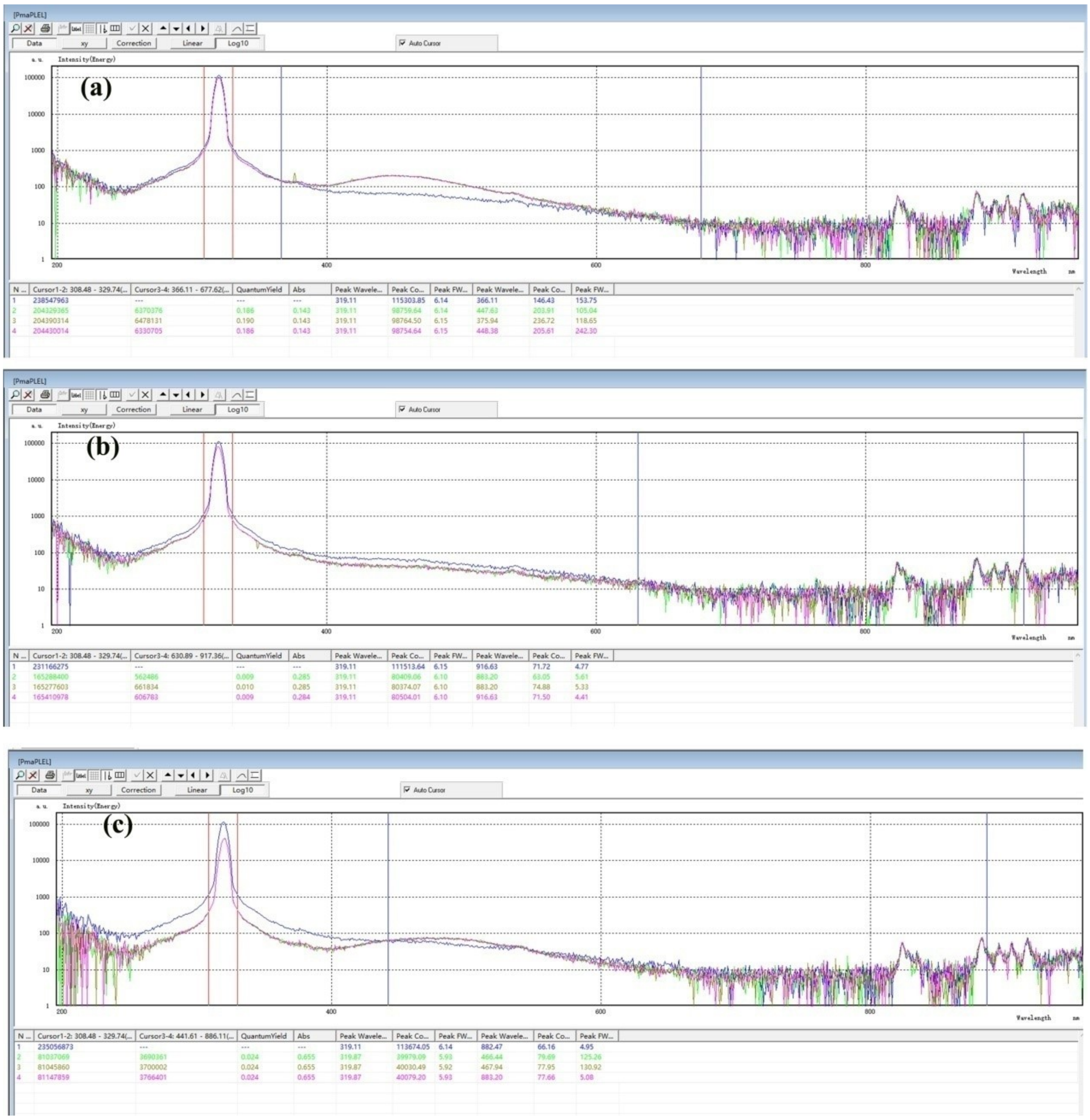

Fig. S7 the quantum yields of **1** and Fe^{3+}@**1** and CrO_4^{2-}@**1**.

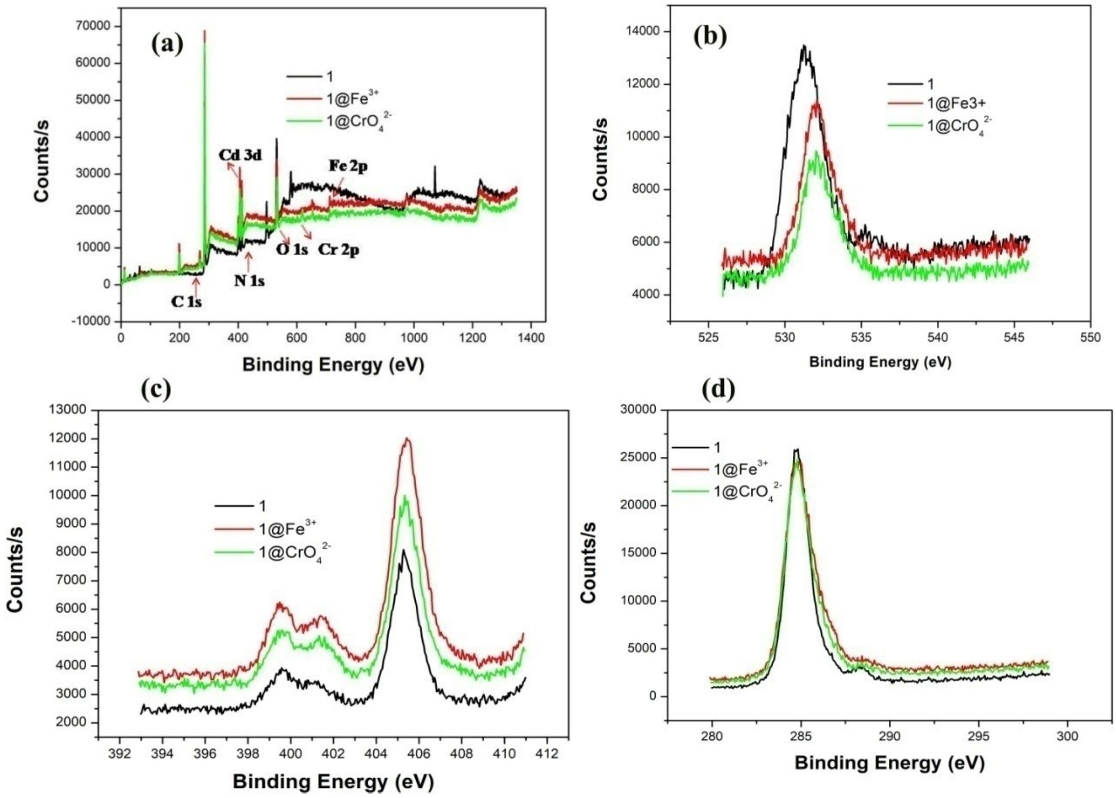

Fig. S8 XPS spectra of **1** before and after the addition of Fe^{3+} and CrO_4^{2-}: (a) full view: (a) O 1s; (b) N 1s and (c) C 1s.

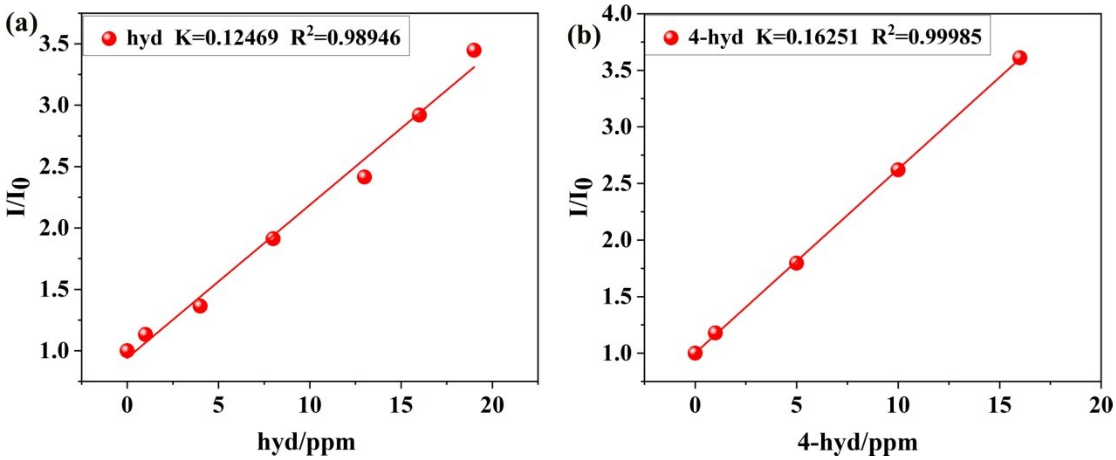

Fig. S9 (a) and (b) The Stern−Volmer (SV) plot of **1**@Fe^{3+} and **1**@CrO_4^{2-} adding hyd and 4-hyd acid, respectively.

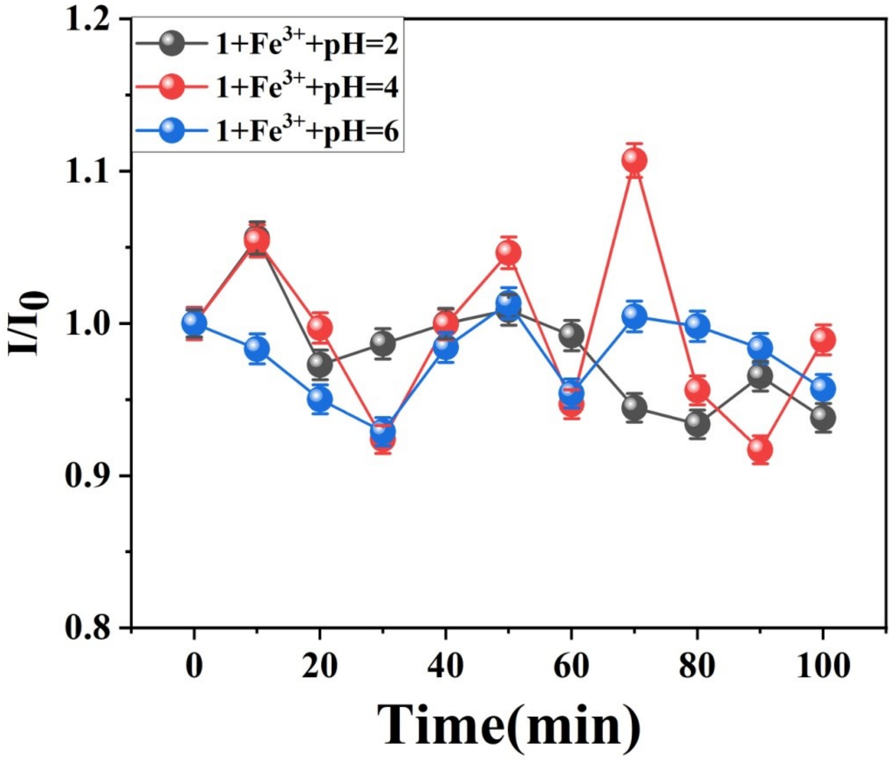

Fig. S10 The Effect of pH (2-6 range) on 1@Fe^{3+} sensor for 100 minutes.

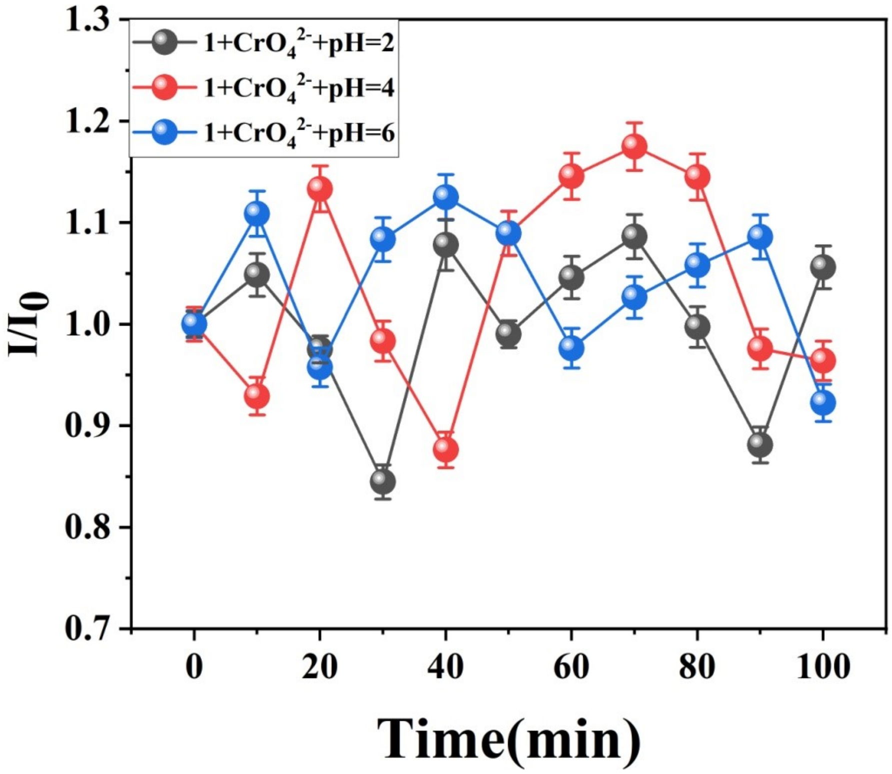

Fig. S11 The Effect of pH (2-6 range) on 1@CrO_4^{2-} sensor for 100 minutes.

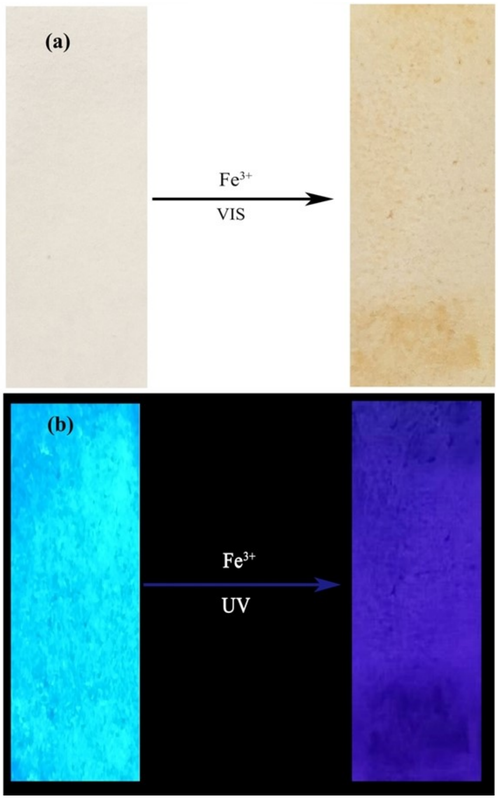

Fig. S12 The color of fluorescent test strips under (a) Visible light and (b) UV-light after addition of 1@Fe^{3+}

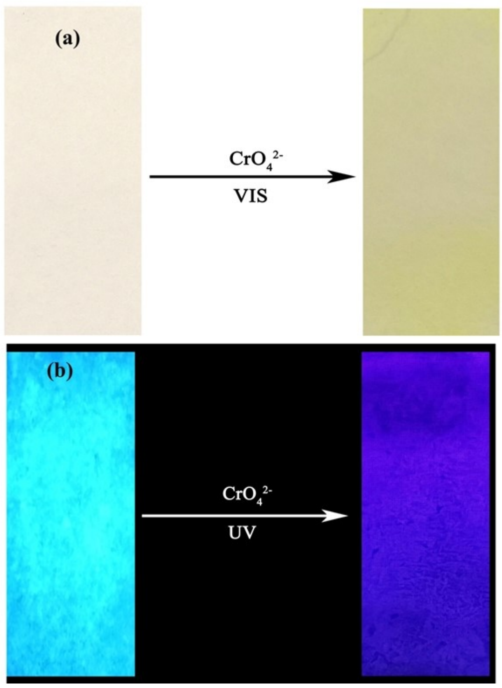

Fig. S13 The color of fluorescent test strips under (a) Visible light and (b) UV-light after addition of 1@CrO_4^{2-}

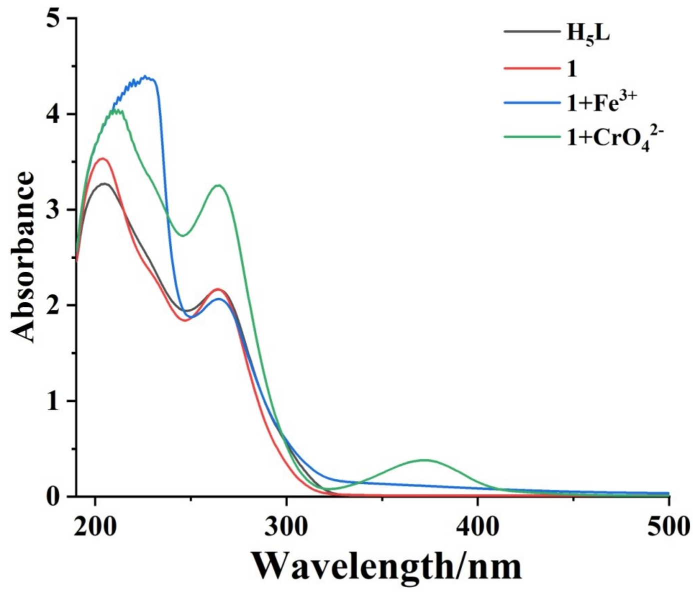

Fig. S14 UV-vis spectra of H_5L, 1, 1+Fe^{3+} and 1+CrO_4^{2-}

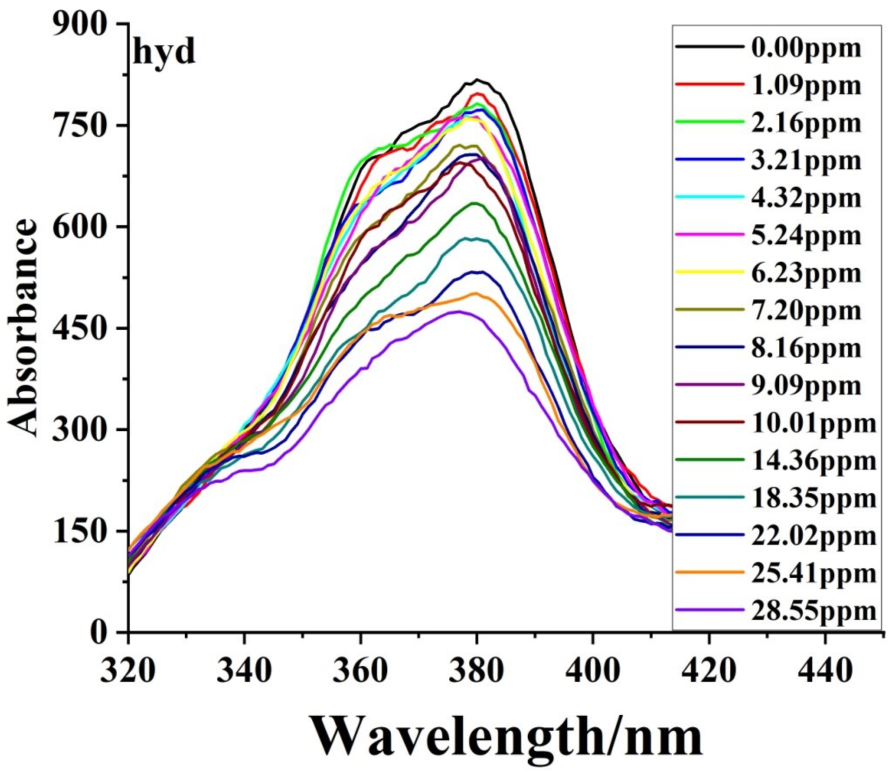

Fig. S15 Sensing studies of hyd using **1**.

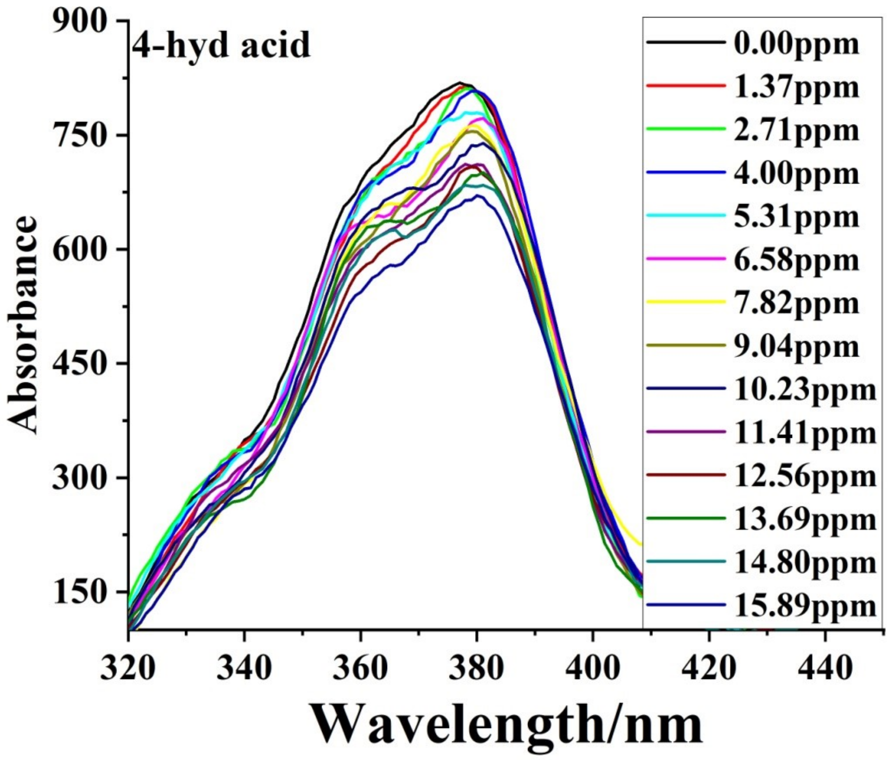

Fig. S16 Sensing studies of 4-hyd acid using **1**.

Table S1 Comparison on the LOD values for Fe^{3+} on MOF-based sensor materials

Entry	material(LCP/LMOF)	Analyte (Fe^{3+})	quenching constant K_{sv}(M^{-1})	LOD (μM)	Media (aqueous/organic)	ref
1	$\{[Tb(L_1)_{1.5}(H_2O)]\cdot 3H_2O\}_n$(Tb-MOF)	Fe^{3+}			DMAc	1
2	$\{[Zn_2(BBIP)_2(NDC)_2]\cdot H_2O\}_n$	Al3^{+}/Ga$_{3+}$	7.21×10^3 /2.75×10^3	6.31×10^{-6} /9.93×10^{-6}		2
3	$\{[Eu_2(MFDA)_2(HCOO)_2(H_2O)_6]\cdot H_2O\}_n$	Fe^{3+}		0.33	CH_3CH_2OH、H_2O、DMF	3
4	$\{[Eu(L)(BPDC)_{1/2}(NO_3)]\cdot H_3O\}$n	Fe^{3+}	5.16×10^4		H_2O	4
	$\{[Tb(L)(BPDC)_{1/2}(NO_3)]\cdot H_3O\}_n$	Fe^{3+}	4.30×10^4		H_2O	4
5	$\{[Co_3(BIBT)_3(BTC)_2(H_2O)_2]\cdot$solvents$\}$n	Fe^{3+}		0.13	CH_3CH_2OH、H_2O、DMA	5
6	$\{[Tb_4(OH)_4(DSOA)_2(H_2O)_8]\cdot(H_2O)_8$	Fe^{3+}	3543		H_2O	6

	}n					
7	$[Zr_6O_4(OH)_8(H_2O)_4(L^1)_2]$	Fe^{3+}	2.17×103	3.8	CH_3COOH、DMF	7
	$[Zr_6O_4(OH)_8(H_2O)_4(L^2)_2]$	Fe^{3+}	1.66×104	0.3	CH_3COOH、DMF	7
8	$[Nd(Hpzbc)_2(NO_3)]\cdot H_2O$ (1-Nd)	Fe^{3+}			CH_3CN	8
	$[Sm(Hpzbc)_2(NO_3)]\cdot H_2O$ (1-Sm)	Fe^{3+}			CH_3CN	8
	$[Eu(Hpzbc)_2(NO_3)]\cdot H_2O$ (1-Eu)	Fe^{3+}		2.6×10^{-5}	CH_3CN	8
	[Gd(Hpzbc)2(NO3)]·H2O (1-Gd)	Fe^{3+}			CH_3CN	8
	$[Tb(Hpzbc)_2(NO_3)]\cdot H_2O$ (1-Tb)	Fe^{3+}			CH_3CN	8
	$[Er(Hpzbc)_2(NO_3)]\cdot H_2O$ (1-Er)	Fe^{3+}			CH_3CN	8
	$[Yb(Hpzbc)_2(NO_3)]\cdot H_2O$ (1-Yb)	Fe^{3+}			CH_3CN	8
9	$[(CH3)_2NH_2]\cdot[Tb(bptc)]\cdot$xsolvents	Fe^{3+}		0.1801	DMF、EtOH、H_2O、HAC	9
10	LCU-10_3	Cu2+/Fe^{3+}	8.48×10^3 /1.79×10^4	1.66/1.45	H2O	10
11	$[Zn_5(hfipbb)_4(trz)_2(H_2O)_2]$	Fe^{3+}		0.20	H_2O、DMF	11
12	Eu-MOF	Fe^{3+}	2.028×10^4		H_2O	12
	Tb-MOF	Fe^{3+}	1.204×10^4		H_2O	12
13	$[Tb_4(\mu_6\text{-}L)_2(\mu\text{-}HCOO)(\mu_3\text{-}OH)_3(\mu_3\text{-}O)(DMF)_2(H_2O)_4]_n\cdot(H_2O)_{4n}$	Fe^{3+}	16590		DMF、H_2O	13
	$[Eu_4(\mu_6\text{-}L)_2(\mu\text{-}HCOO)(\mu_3\text{-}OH)_3(\mu_3\text{-}O)(DMF)_2(H_2O)_4]_n\cdot(H_2O)_{4n}$	Fe^{3+}			DMF、H_2O	13
	$[Gd_4(\mu_6\text{-}L)_2(\mu\text{-}HCOO)(\mu_3\text{-}OH)_3(\mu_3\text{-}O)(DMF)_2(H_2O)_4]_n\cdot(H_2O)_{5n}$	Fe^{3+}			DMF、H_2O	13
	$[Dy_4(\mu_6\text{-}L)_2(\mu\text{-}HCOO)(\mu_3\text{-}$	Fe^{3+}			DMF、H_2O	13

	OH)$_3$(μ$_3$-O)(DMF)$_2$(H$_2$O)$_4$]$_n$·(H$_2$O)$_{4n}$					
	[Er$_4$(μ$_6$-L)$_2$(μ-HCOO)(μ$_3$-OH)$_3$(μ$_3$-O)(DMF)$_2$(H$_2$O)$_4$]$_n$·(H$_2$O)$_{5n}$	Fe^{3+}			DMF、H_2O	13
14	[Tb(TATAB)(H$_2$O)]·$_2$H$_2$O	Fe^{3+}	12.5× 10^4	0.0221	H_2O、NaOH	14
15	MIL-53(Al).	Fe^{3+}		0.9	H_2O	15
	MIL-53(Fe).	Fe^{3+}			DMF、HF	15
16	Eu-MOF	H_2O_2/glucose.		0.0335/0.0643	DMF、H_2O	16
	Tb-MOF	H_2O_2/glucose			DMF、H_2O	16
17	NTU-9-NS	Fe^{3+}		0.45	CH_3COOH	17

[1] Cao LH, Shi F, Zhang WM, Zang SQ, Mak TCW. Selective Sensing of Fe3+ and Al3+ Ions and Detection of 2,4,6-Trinitrophenol by a Water-Stable Terbium-Based Metal–Organic Framework. Chemistry – A European Journal. 2015;21(44):15705-12.

[2] Wu L, Yao S, Xu H, Zheng T, Liu S, Chen J, et al. Highly selective and turn-on fluorescence probe with red shift emission for naked-eye detecting Al3+ and Ga3+ based on metal-organic framework. Chinese Chemical Letters. 2022;33(1):541-6.

[3] Zhou X-H, Li L, Li H-H, Li A, Yang T, Huang W. A flexible Eu(iii)-based metal–organic framework: turn-off luminescent sensor for the detection of Fe(iii) and picric acid. Dalton Transactions. 2013;42(34).

[4] Yan W, Zhang C, Chen S, Han L, Zheng H. Two Lanthanide Metal–Organic Frameworks as Remarkably Selective and Sensitive Bifunctional Luminescence Sensor for Metal Ions and Small Organic Molecules. ACS Applied Materials & Interfaces. 2017;9(2):1629-34.

[5] Tian X-M, Yao S-L, Qiu C-Q, Zheng T-F, Chen Y-Q, Huang H, et al. Turn-On Luminescent Sensor toward Fe3+, Cr3+, and Al3+ Based on a Co(II) Metal–Organic Framework with Open Functional Sites. Inorganic Chemistry. 2020;59(5):2803-10.

[6] Dong X-Y, Wang R, Wang J-Z, Zang S-Q, Mak TCW. Highly selective Fe3+ sensing and proton conduction in a water-stable sulfonate–carboxylate Tb–organic-framework. Journal of Materials Chemistry A. 2015;3(2):641-7.

[7] Wang B, Yang Q, Guo C, Sun Y, Xie L-H, Li J-R. Stable Zr(IV)-Based Metal–Organic Frameworks with Predesigned Functionalized Ligands for Highly Selective Detection of Fe(III) Ions in Water. ACS Applied Materials & Interfaces. 2017;9(11):10286-95.

[8] Li G-P, Liu G, Li Y-Z, Hou L, Wang Y-Y, Zhu Z. Uncommon Pyrazoyl-Carboxyl Bifunctional Ligand-Based Microporous Lanthanide Systems: Sorption and Luminescent Sensing Properties. Inorganic Chemistry. 2016;55(8):3952-9.
[9] Zhao X-L, Tian D, Gao Q, Sun H-W, Xu J, Bu X-H. A chiral lanthanide metal–organic framework for selective sensing of Fe(iii) ions. Dalton Transactions. 2016;45(3):1040-6.
[10] Li Y-W, Li J, Wan X-Y, Sheng D-F, Yan H, Zhang S-S, et al. Nanocage-Based N-Rich Metal–Organic Framework for Luminescence Sensing toward Fe3+ and Cu^{2+} Ions. Inorganic Chemistry. 2021;60(2):671-81.
[11] Hou B-L, Tian D, Liu J, Dong L-Z, Li S-L, Li D-S, et al. A Water-Stable Metal–Organic Framework for Highly Sensitive and Selective Sensing of Fe3+ Ion. Inorganic Chemistry. 2016;55(20):10580-6.
[12] Yu H, Fan M, Liu Q, Su Z, Li X, Pan Q, et al. Two Highly Water-Stable Imidazole-Based Ln-MOFs for Sensing Fe3+,Cr2O72–/CrO42– in a Water Environment. Inorganic Chemistry. 2020;59(3):2005-10.
[13] Zhang Q, Wang J, Kirillov AM, Dou W, Xu C, Xu C, et al. Multifunctional Ln–MOF Luminescent Probe for Efficient Sensing of Fe3+, Ce3+, and Acetone. ACS Applied Materials & Interfaces. 2018;10(28):23976-86.
[14] Wei JH, Yi JW, Han ML, Li B, Liu S, Wu YP, et al. A Water-Stable Terbium(III)–Organic Framework as a Chemosensor for Inorganic Ions, Nitro-Containing Compounds and Antibiotics in Aqueous Solutions. Chemistry – An Asian Journal. 2019;14(20):3694-701.
[15] Yang C-X, Ren H-B, Yan X-P. Fluorescent Metal–Organic Framework MIL-53(Al) for Highly Selective and Sensitive Detection of Fe3+ in Aqueous Solution. Analytical Chemistry. 2013;85(15):7441-6.
[16] Cui Y, Chen F, Yin X-B. A ratiometric fluorescence platform based on boric-acid-functional Eu-MOF for sensitive detection of H2O2 and glucose. Biosensors and Bioelectronics. 2019;135:208-15.
[17] Xu H, Gao J, Qian X, Wang J, He H, Cui Y, et al. Metal–organic framework nanosheets for fast-response and highly sensitive luminescent sensing of Fe^{3+}. Journal of Materials Chemistry A. 2016;4(28):10900-5.

Table S2 Comparison on the LOD value for CrO_4^{2-} on MOF-based sensor materials

entry	material(LCP/LMOF)	analyte(CrO_4^{2-}/$Cr_2O_7^{2-}$)	quenching constant $K_{sv}(M^{-1})$	LOD (μM)	media(aqueous/organic)	ref
1	{[Zn(IPA)(L)]}n (CP1)	CrO_4^{2-} /$Cr_2O_7^{2-}$	1.00×10^3 /1.37×10^3	18.33 /12.02	H_2O	1
	{[Cd(IPA)(L)]}n (CP2)	CrO_4^{2-} /$Cr_2O_7^{2-}$	1.30×10^3 /2.91×10^3	2.52 /2.26	H_2O	1
2	{[Zn_2(tpeb)$_2$(2,5-tdc)(2,5-Htdc)$_2$	Cr^{3+}/CrO_4^{2-} /$Cr_2O_7^{2-}$			H_2O、MeCN	2

	]·$2H_2O$ }$_n$					
	{[Zn_2(tpeb)$_2$(1,4-ndc)(1,4-Hndc)$_2$]·$2.6H_2O$ }$_n$	Cr^{3+}/CrO_4^{2-}/$Cr_2O_7^{2-}$			H_2O、MeCN	2
	{[Zn_2(tpeb)$_2$(2,3-ndc)$_2$]·H_2O}$_n$	Cr^{3+}/CrO_4^{2-}/$Cr_2O_7^{2-}$		0.88/1.734/2.623	H_2O、MeCN	2
3	Eu-MOF	CrO_4^{2-}/$Cr_2O_7^{2-}$	1.91×10^4/1.141×10^4		H_2O	3
	Tb-MOF	CrO_4^{2-}/$Cr_2O_7^{2-}$	1.14×10^4/8.23×10^3		H_2O	3
4	Th-BCTPE-1	CrO_4^{2-}/$Cr_2O_7^{2-}$	2.4×10^5/4.6×10^5	9.0/4.6	DMF、MeOH、CF_3COOH	4
	Th-BCTPE-2	CrO_4^{2-}/$Cr_2O_7^{2-}$	1.30×10^5/2.222×10^5	159/94	DMF、HNO_3	4
5	{[Zn(BBDF)(ATP)]·2DMF·$3H_2O$}$_n$	CrO_4^{2-}/$Cr_2O_7^{2-}$	2.52×10^4/2.64×10^4	0.21/0.17	DMF、H_2O	5
6	{Zn(L)(TPA)·H_2O}n	CrO_4^{2-}/$Cr_2O_7^{2-}$			(CH3)$_2$CHOH、H_2O	6
7	{[Co(L)(bibp)]}n	CrO_4^{2-}/$Cr_2O_7^{2-}$	2.02×10^4/5.74×10^4	1.48/0.52	DMF、H_2O	7
	{[Co(L)(bpy)(H_2O)]$_2$·$2H_2O$}$_n$	CrO_4^{2-}/$Cr_2O_7^{2-}$	1.39×10^4/1.09×10^4	2.15/2.75	DMF、H_2O	7
	{[Co(L)(bipd)]}$_n$	CrO_4^{2-}/$Cr_2O_7^{2-}$	3.25×10^4/3.28×10^4	0.92/0.91	DMAc、H_2O	7
	{[Co(L)(bbibp)]·H_2O}$_n$	CrO_4^{2-}/$Cr_2O_7^{2-}$	1.53×10^4/2.18×10^4	1.96/1.37	DMAc、H_2O	7
8	{[Zn_2L_2(DPA)$_2$]·$3H_2O$}$_n$	CrO_4^{2-}/$Cr_2O_7^{2-}$	1.43×10^4/3.89×10^4	0.71/0.27	DMF、MeOH	8
9	Zr(IV)-MOF(HBU-20)	CrO_4^{2-}/$Cr_2O_7^{2-}$	6.89×10^5/4.75×10^6	0.065/0.0089	DMF、HAC	9
10	Hf-BITD	CrO_4^{2-}/$Cr_2O_7^{2-}$	5.5×10^4/9.5×10^4	0.38/0.33	DMF、HCOOH	10
11	[Zn(L_1)hfdba]$_n$	CrO_4^{2-}/$Cr_2O_7^{2-}$	2.2387×10^3/5.029×10^3	0.745/0.33	DMF、H_2O	11
	{[Zn(L_2)(hfdba)$_2$]·$2H_2O$}$_n$	CrO_4^{2-}/$Cr_2O_7^{2-}$	9.7079×10^3/1.3268×10^4	114.2/83.5	DMF、H_2O	11
12	[Zn(BTA)$_2$]$_n$	$Cr_2O_7^{2-}$	2.69×10^4	5.68×10^{-6}	DMF、H_2O	12
	[Zn_3(BTA)$_2$(5-tbuip)$_2$]$_n$	$Cr_2O_7^{2-}$	1.26×10^4	9.81×10^{-6}	CH3CN、H_2O	12
13	{[Zn(L)$_{0.5}$(bpea)]·$0.5H_2O$·0.5DMF}n	CrO_4^{2-}/$Cr_2O_7^{2-}$	1.34×104/1.65×104	2.65/1.42	DMF、H_2O	13
	{[Zn-	CrO_4^{2-}	1.26×104	3.78/2.21	DMF、H_2O	13

	(L)$_{0.5}$(ibpt)]·H_2O·DMF}n	/$Cr_2O_7^{2-}$	/1.02 × 104			
14	Zn-db-1	CrO_4^{2-} /$Cr_2O_7^{2-}$			2-methoxyethanol、MeOH、H_2O	14
	Zn-db-2	CrO_4^{2-} /$Cr_2O_7^{2-}$			2-methoxyethanol、MeOH、H_2O	14
	Zn-db-3	CrO_4^{2-} /$Cr_2O_7^{2-}$			2-methoxyethanol、MeOH、H_2O	14
15	{[Ln(L)(H_2O)]$_4$$H_2$O}n (Ln = Eu, Tb, Gd)	CrO_4^{2-} /$Cr_2O_7^{2-}$	1.35×10^4 /2.55×10^4	0.79/0.42	H_2O	15
16	{[Zn2(OH)(1,4-ndc)$_{1.5}$(Cz-3,6-bpy)]·2H_2O}n	CrO_4^{2-} /$Cr_2O_7^{2-}$	9.08×10^3 /1.17×10^4	1.10/1.77	DMF	16
17	[Cd(4-bmnpd)(2-NBA)$_2$]	CrO_4^{2-} /$Cr_2O_7^{2-}$	4.447×10^4 /3.180×10^4	6.9×10^{-5} /1.0×10^{-4}	H_2O、NaOH	17
	[Cd(4-bmnpd)(3-NIP).H_2O)]	CrO_4^{2-} /$Cr_2O_7^{2-}$	3.111×10^4 /3.202×10^4	9.6×10^{-5} /9.7×10^{-5}	H_2O、NaOH	17
	[Cd2(4-bmnpd)(TCPA)$_2$]	CrO_4^{2-} /$Cr_2O_7^{2-}$	3.949×10^4 /2.313×10^4	7.5×10^{-5} /1.3×10^{-4}	H_2O、NaOH	17
	[Cd(4-bmnpd)(5-HIP).H_2O)]	CrO_4^{2-} /$Cr_2O_7^{2-}$	3.245×10^4 /2.351×10^4	9.2×10^{-5} /1.3×10^{-4}	H_2O、NaOH	17
	[Cd(4-bmnpd)$_{0.5}$(5-MIP)H_2O)]	CrO_4^{2-} /$Cr_2O_7^{2-}$	3.245×10^4 /3.474×10^4	9.6×10^{-5} /8.6×10^{-5}	H_2O、NaOH	17
	[Cd_3O)4-bmnpd)(1,4-PHDA)$_2$。H_2O)]·H_2O	CrO_4^{2-} /$Cr_2O_7^{2-}$	4.229×10^4 /2.475×10^4	7.1×10^{-5} /1.2×10^{-4}	H_2O、NaOH	17
	[ZnIJ4-bmnpd)-MIP)]	CrO_4^{2-} /$Cr_2O_7^{2-}$	3.022×10^4 /3.915×10^4	1.3×10^{-4} /7.7×10^{-5}	H_2O、NaOH	17
	[Zn(4-bmnpd)(1,2,4,5-BTA)]·H_2O	CrO_4^{2-} /$Cr_2O_7^{2-}$	2.317×10^4 /2.323×10^4	1.0×10^{-4} /1.3×10^{-4}	H_2O、NaOH	17

[1] Parmar B, Rachuri Y, Bisht KK, Laiya R, Suresh E. Mechanochemical and Conventional Synthesis of Zn(II)/Cd(II) Luminescent Coordination Polymers: Dual

Sensing Probe for Selective Detection of Chromate Anions and TNP in Aqueous Phase. Inorganic Chemistry. 2017;56(5):2627-38.
[2] Gu T-Y, Dai M, Young DJ, Ren Z-G, Lang J-P. Luminescent Zn(II) Coordination Polymers for Highly Selective Sensing of Cr(III) and Cr(VI) in Water. Inorganic Chemistry. 2017;56(8):4668-78.
[3] Yu H, Fan M, Liu Q, Su Z, Li X, Pan Q, et al. Two Highly Water-Stable Imidazole-Based Ln-MOFs for Sensing Fe3+,Cr2O72–/CrO42– in a Water Environment. Inorganic Chemistry. 2020;59(3):2005-10.
[4] Li Z-J, Ju Y, Wu X-L, Li X, Qiu J, Li Y, et al. Topological control of metal–organic frameworks toward highly sensitive and selective detection of chromate and dichromate. Inorganic Chemistry Frontiers. 2023;10(6):1721-30.
[5] Li C, Sun X, Meng X, Wang D, Zheng C. A water stable and highly fluorescent Zn(ii) based metal–organic framework for fast detection of Hg2+, CrVI, and antibiotics. Dalton Transactions. 2023;52(22):7611-9.
[6] Zhang J, Chen L, Chen Q, Yue Y, Chen Q, Yin D, et al. An efficient dual-response luminescent metal-organic framework sensor constructed by new photochromic ligand. Dyes and Pigments. 2023;220.
[7] Luo R, Xu C, Chen G, Xie C-Z, Chen P, Jiang N, et al. Four Novel Cobalt(II) Coordination Polymers Based on Anthracene-Derived Dicarboxylic Acid as Multi-functional Fluorescent Sensors toward Different Inorganic Ions. Crystal Growth & Design. 2023;23(4):2395-405.
[8] Mondal S, Sahoo R, Das MC. pH-Stable Zn(II) Coordination Polymer as a Multiresponsive Turn-On and Turn-Off Fluorescent Sensor for Aqueous Medium Detection of Al(III) and Cr(VI) Oxo-Anions. Inorganic Chemistry. 2023;62(34):14124-33.
[9] Ren Y-B, Xu H-Y, Yan J-W, Cao D-X, Du J-L. Multifunctional luminescent Zr(IV)-MOF for rapid and efficient detection of vanillin, CrO42- and Cr2O72- ions. Spectrochimica Acta Part A: Molecular and Biomolecular Spectroscopy. 2022;278.
[10] Wang X, Li Z-J, Ju Y, Li X, Qian J, He M-Y, et al. A MOF-based luminometric sensor for ultra-sensitive and highly selective detection of chromium oxyanions. Talanta. 2023;252.
[11] Pal SC, Mukherjee D, Das MC. pH-Stable Luminescent Metal–Organic Frameworks for the Selective Detection of Aqueous-Phase FeIII and CrVI Ions. Inorganic Chemistry. 2022;61(31):12396-405.
[12] Shao J-J, Ni J-L, Liang Y, Li G-J, Chen L-Z, Wang F-M. Luminescent MOFs for selective sensing of Ag+ and other ions (Fe(iii) and Cr(vi)) in aqueous solution. CrystEngComm. 2022;24(13):2479-84.
[13] Xian G, Wang L, Wan X, Yan H, Cheng J, Chen Y, et al. Two Multiresponsive Luminescent Zn-MOFs for the Detection of Different Chemicals in Simulated Urine and Antibiotics/Cations/Anions in Aqueous Media. Inorganic Chemistry. 2022;61(19):7238-50.
[14] Ghosh A, Sikdar N, Maji TK. An excited-state intramolecular proton-transfer responsive nanoscale MOF for dual sensing of water and chromate ions. Journal of Materials Chemistry C. 2022;10(19):7558-66.

[15] Li B, Dong J-P, Zhou Z, Wang R, Wang L-Y, Zang S-Q. Robust lanthanide metal–organic frameworks with "all-in-one" multifunction: efficient gas adsorption and separation, tunable light emission and luminescence sensing. Journal of Materials Chemistry C. 2021;9(10):3429-39.
[16] Chuang P-M, Wu J-Y. A highly stable Zn coordination polymer exhibiting pH-dependent fluorescence and as a visually ratiometric and on–off fluorescent sensor. CrystEngComm. 2021;23(30):5226-40.
[17] Chen Y, Liu G, Wang X, Lu X, Xu N, Chang Z, et al. Various carboxylates induced eight Zn(ii)/Cd(ii) coordination polymers with fluorescence sensing activities for Fe(iii), Cr(vi) and oxytetracycline. CrystEngComm. 2021;23(46):8077-86.

Table S3 Crystallographic data and structure refinement details for 1

Parameter	1
Formula	$C_{76}H_{62}Cd_3N_8O_{20}$
Formula weight	1744.53
Crystal system	Triclinic
Space group	P-1
a, Å	13.3139(6)
b, Å	13.6689(6)
c, Å	19.2341(9)
α, °	86.6362(8)
β, °	88.2811(8)
γ, °	76.7955(7)
V, Å ^{3}	3401.4(3)
Z	2
ρ_{calcd}, g/cm^3	1.199
μ, mm^{-1}	1.015
F(000)	1196
θ Range, deg	2.5-27.7
Reflection Collected	20808
Independent reflections (R_{int})	0.0162
Reflections with $I > 2\sigma(I)$	14911
Number of parameters	622
R_1, wR_2 ($I > 2\sigma(I)$)*	0.0287，0.0715

R_1, wR_2 (all data)**	0.0375，0.0750

* $R = \sum(F_o - F_c)/\sum(F_o)$, ** $wR_2 = \{\sum[w(F_{O(2)} - F_c^2)^2]/\sum(F_{O(2)})^2\}^{1/2}$.

Table S4. Selected bond distances (Å) and angles (deg) for **1**

	1		
Cd(1)-O(1)	2.509(3)	Cd(1)-O(2)	2.331(2)
Cd(1)-O(7)	2.217(2)	Cd(1)-O(19)#2	2.393(2)
Cd(1)-O(20)#2	2.292(2)	Cd(1)-O(9)#6	2.2609(19)
Cd(2)-O(3)	2.187(2)	Cd(2)-O(15)#4	2.524(2)
Cd(2)-O(16)#4	2.439(3)	Cd(2)-O(17)#4	2.606(2)
Cd(2)-O(18)#4	2.267(2)	Cd(2)-O(13)#5	2.3007(16)
Cd(2)-O(5)#7	2.5370(19)	Cd(3)-O(5)	2.4988(18)
Cd(3)-O(6)	2.2965(18)	Cd(3)-O(11)	2.401(2)
Cd(3)-O(12)	2.311(2)	Cd(3)-O(10)#1	2.2487(18)
Cd(3)-O(13)#3	2.5859(17)	Cd(3)-O(14)#3	2.2902(19)
	1		
O(1)-Cd(1)-O(2)	53.70(8)	O(3)-Cd(2)-O(15)#4	91.99(8)
O(1)-Cd(1)-O(7)	82.85(8)	O(3)-Cd(2)-O(16)#4	133.34(8)
O(3)-Cd(2)-O(17)#4	152.33(7)	O(3)-Cd(2)-O(18)#4	111.88(8)
O(1)-Cd(1)-O(19)#2	111.34(8)	O(1)-Cd(1)-O(20)#2	90.43(8)
O(3)-Cd(2)-O(13)#5	86.60(7)	O(15)#4-Cd(2)-O(17)#4	108.59(8)
O(1)-Cd(1)-O(9)#6	141.47(7)	O(3)-Cd(2)-O(5)#7	83.80(7)
O(2)-Cd(1)-O(7)	98.28(8)	O(15)#4-Cd(2)-O(16)#4	50.94(8)
O(2)-Cd(1)-O(19)#2	163.64(8)	O(15)#4-Cd(2)-O(18)#4	87.88(8)
O(2)-Cd(1)-O(20)#2	114.07(7)	O(13)#5-Cd(2)-O(15)#4	107.19(7)
O(2)-Cd(1)-O(9)#6	90.17(7)	O(5)#7-Cd(2)-O(15)#4	174.86(7)
O(16)#4-Cd(2)-O(17)#4	74.15(7)	O(7)-Cd(1)-O(19)#2	85.02(7)
O(16)#4-Cd(2)-O(18)#4	95.85(8)	O(7)-Cd(1)-O(20)#2	133.80(8)
O(13)#5-Cd(2)-O(16)#4	80.56(7)	O(7)-Cd(1)-O(9)#6	119.28(8)
O(5)#7-Cd(2)-O(16)#4	134.19(7)	O(17)#4-Cd(2)-O(18)#4	52.78(7)
O(13)#5-Cd(2)-O(17)#4	103.96(6)	O(5)#7-Cd(2)-O(17)#4	74.50(6)
O(19)#2-Cd(1)-O(20)#2	55.16(7)	O(13)#5-Cd(2)-O(18)#4	156.10(7)
O(9)#6-Cd(1)-O(19)#2	102.25(7)	O(5)#7-Cd(2)-O(18)#4	90.96(7)
O(9)#6-Cd(1)-O(20)#2	93.72(8)	O(5)#7-Cd(2)-O(13)#5	75.58(6)
O(5)-Cd(3)-O(6)	53.99(6)	O(5)-Cd(3)-O(11)	130.28(8)
O(5)-Cd(3)-O(12)	95.10(7)	O(5)-Cd(3)-O(10)#1	143.78(7)
O(10)#1-Cd(3)-O(13)#3	130.45(6)	O(5)-Cd(3)-O(13)#3	71.46(6)
O(10)#1-Cd(3)-O(14)#3	82.82(7)	O(5)-Cd(3)-O(14)#3	96.56(7)
O(13)#3-Cd(3)-O(14)#3	53.26(6)	O(6)-Cd(3)-O(11)	166.80(8)
O(6)-Cd(3)-O(12)	114.59(7)	O(6)-Cd(3)-C(15)	26.91(7)
O(6)-Cd(3)-C(24)	141.31(8)	O(6)-Cd(3)-O(13)#3	113.04(6)
O(6)-Cd(3)-O(14)#3	94.90(7)	O(11)-Cd(3)-O(12)	55.01(7)
O(10)#1-Cd(3)-O(11)	85.42(8)	O(11)-Cd(3)-O(13)#3	79.12(7)

O(11)-Cd(3)-O(14)#3	96.74(7)	O(10)#1-Cd(3)-O(12)	103.57(7)
O(12)-Cd(3)-O(13)#3	105.06(6)	O(12)-Cd(3)-O(14)#3	149.57(7)

Symmetry Codes:#1=x,-1+y,z；#2=x,1+y,1+z；#3=1+x,y,z；#4=1+x,y,1+z；#5=-x,1-y,1-z；#6=-x,2-y,1-z；#7=1-x,1-y,1-z；